

Star Formation Rates in [Ne v] 3426 Å Selected Active Galactic Nuclei: Evidence for a Decrease along the Main Sequence?

LÉA M. FEUILLET ¹, MARCIO MELÉNDEZ ², STEVE KRAEMER ¹, HENRIQUE R. SCHMITT ³, TRAVIS C. FISCHER ⁴,
AND JAMES N. REEVES ¹

¹*Institute for Astrophysics and Computational Sciences, Department of Physics, The Catholic University of America, Washington, DC 20064, USA*

²*Space Telescope Science Institute, 3700 San Martin Drive Baltimore, MD 21218, USA*

³*Naval Research Laboratory, Remote Sensing Division, 4555 Overlook Ave SW, Washington, DC 20375, USA*

⁴*AURA for ESA, Space Telescope Science Institute, 3700 San Martin Drive, Baltimore, MD 21218, USA*

(Accepted May 7, 2024)

ABSTRACT

Studying the behavior along the galaxy main sequence is key in furthering our understanding of the possible connection between AGN activity and star formation. We select a sample of 1215 AGN from the catalog of SDSS galaxy properties from the Portsmouth group by detection of the high-ionization [Ne v] 3426 Å emission line. Our sample extends from 10^{40} to $10^{42.5}$ erg/s in [Ne v] luminosity in a redshift range $z = 0.17$ to 0.57 . We compare the specific star formation rates (sSFRs, SFR scaled by galaxy mass) obtained from the corrected [O II] and $H\alpha$ luminosities, and the SED-determined values from Portsmouth. We find that the emission-line-based sSFR values are unreliable for the [Ne v] sample due to the AGN contribution, and proceed with the SED sSFRs for our study of the main sequence. We find evidence for a decrease in sSFR along the main sequence in the [Ne v] sample which is consistent with results from the hard X-ray BAT AGN sample, which extends to lower redshifts than our [Ne v] sample. Although we do not find evidence that the concurrent AGN activity is suppressing star formation, our results are consistent with a lower gas fraction in the host galaxies of the AGN as compared to that of the star forming galaxies. If the evacuation of gas, and therefore suppression of star formation is due to AGN activity, it must have occurred in a previous epoch.

Keywords: Active Galaxies (17) — Starburst galaxies (1570) — Star formation (1569)

1. INTRODUCTION

The main sequence (MS; Noeske et al. 2007) for star-forming galaxies (SFGs) corresponds to the linear correlation between the star formation rate (SFR) and the mass of the galaxy (M_*) in log space. This relationship has been demonstrated extensively and is evident over a range of redshifts, but the correlation varies dramatically between different studies and samples used (see Speagle et al. 2014 for a review).

Additionally, the introduction of active galactic nuclei (AGN) within the sample modifies the behavior of the relationship (e.g. Salim et al. 2007; Shimizu et al. 2015; Mullaney et al. 2015; Stemo et al. 2020). AGN are galaxies containing an accreting supermassive black hole (SMBH) at the center. The presence of this accreting SMBH serves as a powerful source of ionizing radiation which interacts with the ambient gas in the

host galaxy. This ionizing radiation is believed to be responsible for the negative feedback process within the AGN (see Heckman & Best 2014 for a review). Specifically, this radiation would accelerate winds and, in turn, create shocks, which would heat and evacuate the material necessary for star formation from the host galaxy (e.g. Silk & Rees 1998; King 2003; Di Matteo et al. 2005).

The deviation of AGN from the main sequence has been demonstrated by Shimizu et al. (2015) using the *Swift* Burst Alert Telescope (BAT) catalog. The AGN in this sample are hard X-ray selected, which makes it an unambiguous sample of AGN unbiased by the presence of star formation and obscuration. The BAT AGN are local ($z \leq 0.05$), and they analyze their location with respect to the star-forming MS obtained using far-infrared (FIR) emission from *Herschel* data in the same redshift range. They suggest that this reduction in the SFR is

due to AGN feedback which reduces the amount of cold gas that is available for star formation in the AGN. In contrast, our approach consists of using optical data to obtain an unambiguous AGN sample through the use of the [Ne v] 3426 Å emission line. Details regarding our decision to use [Ne v] are given in Section 2. Our data also sample a very different redshift range, which corresponds to a different part of cosmological evolution.

We use optical data from the *Sloan Digital Sky Survey* (SDSS) DR12 galaxy data extracted and made available by the Portsmouth group¹ (Data Release 12; Alam et al. 2015). Although the MPA/JHU DR7² sample is much more widely used than the more recent Portsmouth sample (e.g. Leslie et al. 2016; McPartland et al. 2019; Zhuang & Ho 2019; Torbaniuk et al. 2021), the [Ne v] line is not part of their standard pipeline processing. The SDSS is an optical survey with an extensive galaxy catalog, which allows us to use the [Ne v] optical line to classify our AGN amongst a large initial sample. The Baryon Oscillation Spectroscopic Survey (BOSS) was used to obtain spectral information. Due to the relatively high redshift of the samples used in this paper, the analyzed spectra encompass the entire galaxy, which allows us to take both the host galaxy and the AGN contributions to the emission lines and total spectral energy distributions (SEDs) into account.

This paper is outlined as follows. Section 2 details the selection process used to obtain the samples adopted throughout the paper. In Section 3, we compared three methods of obtaining the SFR for the galaxies in our sample. We then plot our main sequence, which supports the findings of Shimizu et al. (2015) regarding the decrease along the main sequence using a different data set. Finally, we discuss what conclusions can be drawn from the deviation concerning feedback from the AGN to the host galaxy in Section 4. We use *Wilkinson Microwave Anisotropy Probe* (WMAP) 12-year results cosmology throughout, with $H_0 = 70.0 \text{ kms}^{-1} \text{ Mpc}^{-1}$, and $\Omega_0 = 0.721$.

2. SAMPLES AND DATA SELECTION

The sample and data selection process is explained in detail in Feuillet et al. (2024). To summarize, the data in the Portsmouth group’s emissionLinesPort table is used to obtain emission-line equivalent widths (EWs), fluxes and their uncertainties, and redshifts for the galaxies (Thomas et al. 2013). The emission-line fluxes were corrected for interstellar reddening by using the observed and theoretical Balmer decrements ($H\alpha/H\beta$) and the

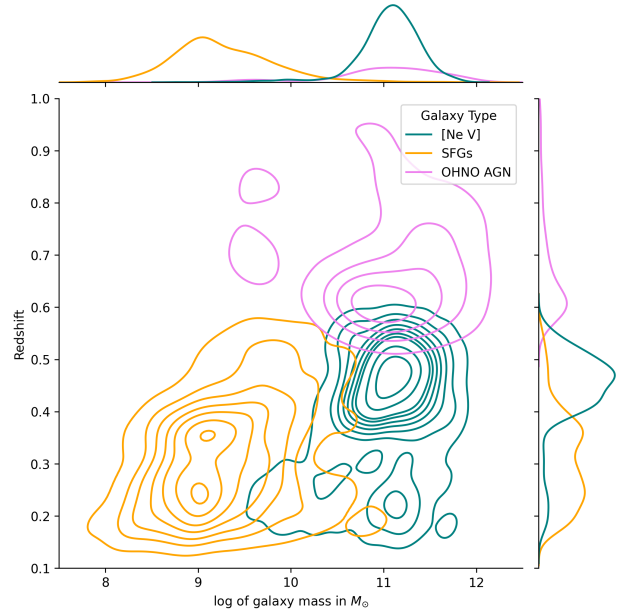


Figure 1. Redshift vs mass distributions for the SFGs, [Ne v] AGN and OHNO classified samples. The redshift was obtained spectroscopically, and the galaxy mass values were calculated using GANDALF (Sarzi et al. 2006) by the Portsmouth group.

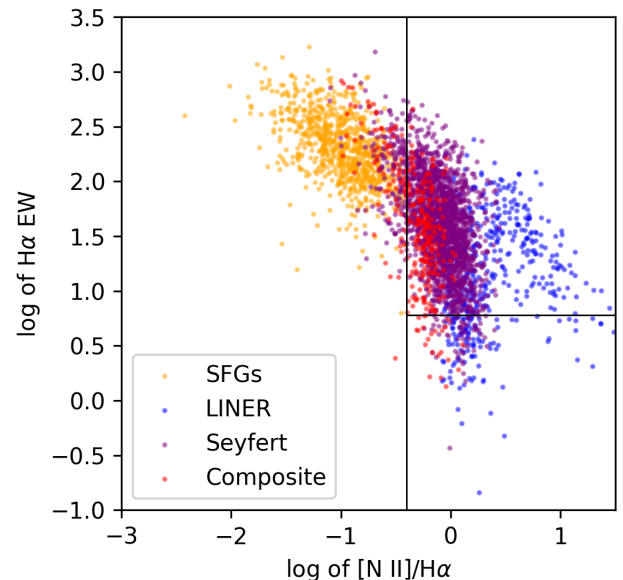


Figure 2. Our [Ne v] AGN and star-forming samples plotted on Cid Fernandes et al. (2011)’s WHAN diagram, demonstrating the reliability of using [Ne v] to select AGN, as 90% are indeed in the AGN region.

Cardelli et al. (1989) reddening law for $R_v = 3.1$, to obtain the $E(B-V)$ values. We also require an $S/N \geq 3$ for the [Ne III] 3869 Å, [O III] 5007 Å, [O II] 3726, 3728 Å, and $H\alpha$ emission-lines (hereafter [Ne III], [O III], and

¹ https://www.sdss.org/dr12/spectro/galaxy_portsmouth/

² <http://www.mpa-garching.mpg.de/SDSS/DR7/>

[O II]). We then separate the galaxies into two samples: the SFGs sample and the full AGN sample, which have been classified using the standard BPT diagram. The [Ne v] sample is a sub-sample of the full AGN sample, corresponding to all AGN with a S/N > 3 for the [Ne v] emission-line flux.

Although the [O III] 5007 Å has been preferred over the [Ne v] 3426 Å line for AGN classification purposes, [Ne v] allows for a greater redshift range (up to $z \leq 2$) when using SDSS and BOSS, despite being weaker. The use of [Ne v] for this purpose has been demonstrated in both the IR (see Abel & Satyapal 2008; Satyapal et al. 2008; Goulding & Alexander 2009) and the optical (e.g. Schmidt et al. (1998), Gilli et al. (2010), and Mignoli et al. (2013)). It has been shown by Baldwin et al. (1981), that none of the HII regions investigated showed any amount of [Ne v] within their spectra, as even the hottest main sequence stars do not emit photons energetic enough to produce [Ne v]. Ne⁺⁴ has a high ionization potential (97 eV), can only be produced by high-energy phenomena such as shocks and the presence of AGN, and is thus an ideal AGN tracer.

In this paper, we make additional use of the stellarMassStarformingPort table which contains the star-formation rates and galaxy masses. Both are calculated by the Portsmouth group through SED fitting, similar to the method used in Shimizu et al. (2015), with models found in Maraston et al. (2006). We direct readers to Maraston et al. (2013) for further information on the determination of stellar masses. We use the values obtained using a Salpeter (1955) initial mass function (IMF) and convert them to a Chabrier IMF using a 0.67 factor throughout the present paper, as suggested in Madau & Dickinson (2014).

The redshift for the [Ne v] sample extends from $0.168 \leq z \leq 0.568$, with galaxy masses ranging within $9.150 \leq \log M_* \leq 11.890$. To compare galaxies at similar redshifts, we limit the SFGs to the same range as the [Ne v] AGN. For comparison with higher redshift galaxies, we use the OHNO diagram presented in Feuillet et al. (2024) to get a sample of AGN that extends to a redshift of 1.07. The full distributions for the redshift and mass of the SFGs, [Ne v] AGN, and OHNO AGN samples are given in Figure 1. We also plot our SFGs and [Ne v] AGN on the WHAN diagram (Cid Fernandes et al. 2011) (see Figure 2). The WHAN diagram plots the H α EW against [N II]/H α , with delimitation lines separating the SFGs from the AGN and Seyfert galaxies from LINERs. 90% of the [Ne v] AGN sample also falls in the AGN region of the WHAN diagram. We will now use our SFGs and AGN samples to investigate the MS.

3. MAIN SEQUENCE

3.1. Star Formation Rates

Determining the SF galaxy MS is dependent on the availability of accurate SFRs, which can be obtained using a variety of methods (see Kennicutt & Evans 2012 for a review). However, the presence of an AGN can influence the resulting SFR values. In the case of SED fitting, the AGN affects the shape of the SED and the light from the AGN can be interpreted as coming from the formation of young stars, thereby increasing the resulting SFR (Pacifci et al. 2023). Ciesla et al. (2015) found that by not omitting an AGN component when using SED fitting to obtain the SFRs of AGN, as is the case for our SED-determined SFRs, the ratios are overestimated³.

When looking at emission-line derived SFR, the results depend on the contribution of the AGN to the total flux observed. Various studies have determined contributions of the AGN to the fluxes of the emission lines used as star formation tracers. For instance, Meléndez et al. (2008) investigated a sample of nearby Seyfert galaxies observed with *Spitzer's* Infrared Spectrograph (IRS). They found that 34-75% of the flux of the IR line [Ne II] 12.81 μm , which has been used as a SFR indicator similar to [O II] (Cao et al. 2008), is due to the presence of the AGN (see also Meléndez et al. 2014). Thomas et al. (2018) also report contributions to the [O II] flux ranging between 20% and 100%, while Davies et al. (2014) found contributions of about 40%. The additional contribution from the AGN thus leads once again to an overestimation of the SFR values.

Evidently, according to the literature, neither SED nor emission-line determined values may give perfect estimates of the SFRs for our AGN. We now compare the different SFR values available for our sample to investigate the biases in further detail. The Portsmouth group provides values for both the SFR and mass by fitting the galaxies' SED using the method described in Maraston et al. (2013). The SDSS spectrum range contains the [O II] and H α emission lines, which we may also use to obtain SFR values.

Kewley et al. (2004) use a sample of purely SFGs, excluding any potential AGN, to derive their [O II]-based SFR equation. The relationship specifically requires the luminosity values to be corrected for reddening. The equation is given as follows:

$$\text{SFR}([\text{O II}]) = (6.58 \pm 1.65) * 10^{-42} L([\text{O II}]) \quad (1)$$

³ Ciesla et al. (2015) also found that the resulting stellar mass estimates were not affected by the inclusion or omission of an AGN component when it comes to type 2 AGN.

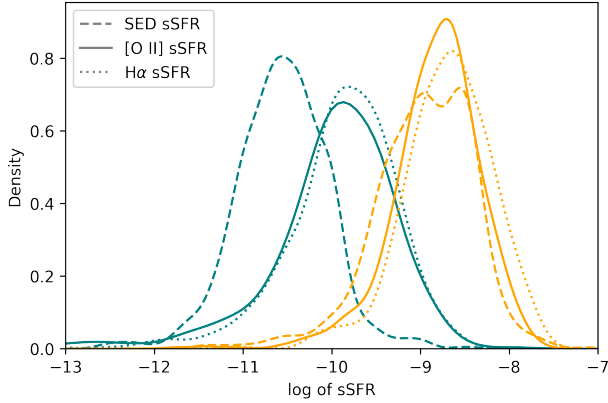


Figure 3. Comparison of the sSFR values from Portsmouth’s SED fitting method to the [O II] emission-line equation from Kewley et al. (2004) and the H α relationship from Kennicutt (1998). We show the distribution of the sSFR values for the [Ne v] AGN (green) and SFG (orange) samples. The [O II] and H α -based values are higher than the SED value because of the contribution to both emission lines by the AGN.

in which $\text{SFR}([\text{O II}])$ is the star formation rate, and $L([\text{O II}])$ is the luminosity of the [O II] emission line (Kewley et al. 2004). Additionally, the H α -based SFR is obtained using:

$$\text{SFR}(\text{H}\alpha) = 7.9 * 10^{-42} L(\text{H}\alpha) \quad (2)$$

in which $\text{SFR}(\text{H}\alpha)$ is the star formation rate, and $L(\text{H}\alpha)$ is the luminosity of the H α emission line (Kennicutt 1998). Using these relationships and the masses obtained by the Portsmouth group, we also define the specific star-formation rate (sSFR), which corresponds to the SFR of a galaxy divided by its total mass.

We obtained sSFR values for our SFGs and [Ne v] AGN samples and plotted the estimated probability density for the results of all three methods (see Figure 3). Looking at the star-forming sSFR distributions, we can see that all three overlap considerably. This suggests that all three methods give similar results when applied to the SFGs. On the other hand, the [Ne v] AGN galaxies show a significant deviation between the SED and the H α and [O II] methods, with the former showing overall lower sSFR values compared to the other two. This is likely due to the aforementioned contribution of the AGN to the emission lines, which does not appear to affect the SED fitting method as significantly. To mitigate the overestimation of the SFR, we proceed with the use the SED SFR and sSFR values to investigate the MS for our samples, with the caveat that there still may be inherent uncertainties due to the presence of the AGN.

3.2. Behavior Along Our Main Sequence

Using the SED-determined SFRs and masses provided by the Portsmouth group, we plot the main sequence for our SFGs. We fit the SFGs using linear regression and find that the equations for our MS is:

$$\log \text{SED SFR} = 0.28 \log M_* - 2.25 \quad (3)$$

We also calculate the standard deviation (σ) for the regression lines⁴, which is $\sigma_{\text{SED}/[\text{O II}]} = 0.39$. The MS regression lines and the $\pm 1\sigma$ lines are all plotted on top of the MS in Figure 4, left panel. We have also plotted the [Ne v] AGN sample on the MS plot, with the deviation already apparent. While the majority of the SFGs are included within 1σ of the MS, the [Ne v] AGN have a significant number falling below in both plots.

We now study the full SFG and [Ne v] AGN samples in more detail, and adopt a similar convention to study the deviation from the main sequence as those of Shimizu et al. (2015). We calculate the distance from our MS as such:

$$\Delta \log M_* = \log \text{SFR}_{\text{SED}} - \log \text{SFR}_{\text{MS}} \quad (4)$$

where $\log \text{SFR}_{\text{SED}}$ is the SED-determined SFR for each galaxy and $\log \text{SFR}_{\text{MS}}$ is the theoretical SFR given by the equation of our MS. The distributions for the resulting values are plotted on the left panel of Figure 4.

Table 1. Summary of the percentages of galaxies below, within, and above the MS defined by the SFGs.

Sample	$\leq -1\sigma$	in MS	$1\sigma \leq$
SFGs	15%	72%	13%
[Ne v]	49%	50%	1%
OHNO	32%	61%	7%

The [Ne v] AGN having approximately half of the population lying below the MS using both SFR options is significant and confirms the deviation from the MS that could already be seen on the scatter plot (see Table 1 for the full description of the values). Once again, as the SED-derived SFRs are likely to be overestimates, it is probable that the true deviation from the MS is even greater than seen in Figure 4. The OHNO AGN have a similar distribution to the [Ne v] AGN when using the SED-determined SFRs, with 32% below the MS, but represent a higher redshift range. This suggests that

⁴ The standard deviation for the regression line is obtained using the following equation: $S_{y/x} = \sqrt{S_r/(n-2)}$, where $S_r = \sum_{i=1}^n (y_i - a_0 - a_1 x_i)^2$ is the sum of squares of the residuals with respect to the regression line, a_0 and a_1 are the intercept and slope of the regression line respectively, and n is the number of data points.

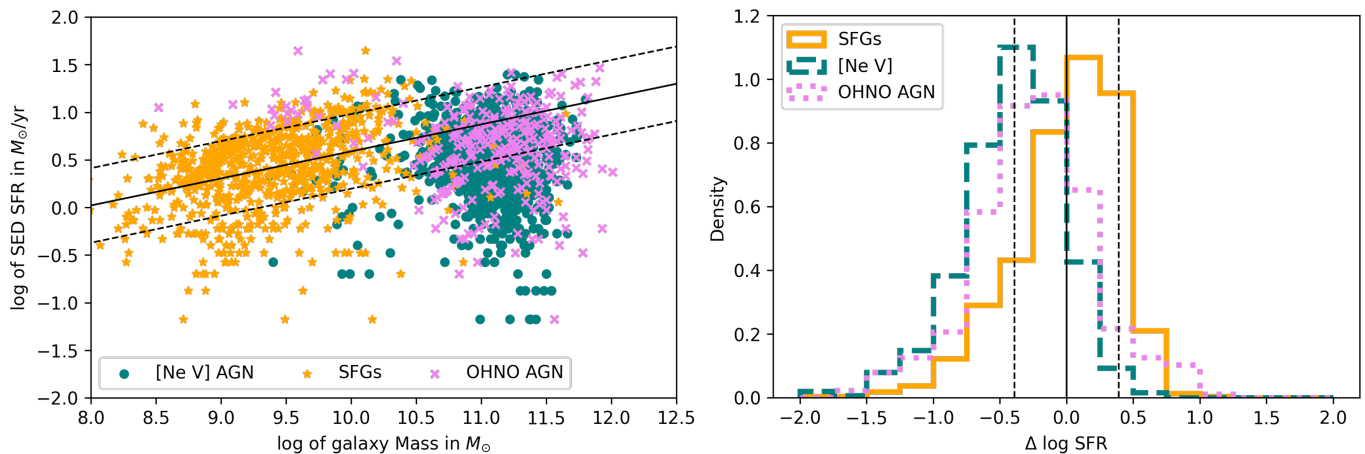


Figure 4. Left panel: Our three samples plotted on the main sequence. The solid black line corresponds to the best fit main sequence for the SFGs, and the dashed ones show the $\pm 1\sigma$ lines. We can see the $[\text{Ne v}]$ AGN falling below the main sequence. Right panel: Distributions showing the distance from the main sequence explicitly for all three samples.

the phenomenon is present at least up to a redshift of 1.06.

3.3. Redshift and Mass Dependence of the Deviation from the MS

It is well known that the SFR has varied since the beginning of the Universe, with a peak in star formation density occurring around $z = 2$ (Madau & Dickinson 2014). While the redshift ranges of the samples overlap as seen in Figure 1, we can also see that the $[\text{Ne v}]$ AGNs are concentrated at a higher redshift compared to the SFG sample. The AGN are therefore closer to the peak in SF, and would therefore tend toward having higher SFRs, which is the opposite of what we have shown in this paper. Additionally, further investigation of the redshift-dependence of the deviation from the MS shows that it is apparent regardless of redshift. As can be seen in Figure 5, the deviation is very clear at all redshift ranges, with the exception of the first where the ambiguity stems from the small $[\text{Ne v}]$ AGN sample size. Hence, we are confident that the deviation from the main sequence is truly the result of AGN activity, as also suggested by Shimizu et al. (2015).

Due to the use of the $[\text{Ne v}]$ emission-line to obtain an unambiguous sample of AGN, our resulting $[\text{Ne v}]$ AGN tend towards having higher masses, as seen in Figure 1. Indeed, the galaxies must be powerful enough to produce a significant amount of $[\text{Ne v}]$ flux for the S/N ratio to be greater than 3, which requires a luminous AGN. AGN luminosity is a function of both the accretion rate and the black hole mass. However, even AGN with sub-Eddington accretion rates such as Mrk 3 (Collins et al. 2009), show strong $[\text{Ne v}]$ provided that they SMBH of sufficient mass. e.g., $> 10^7 M_\odot$. Therefore, given the relationship between bulge mass and the

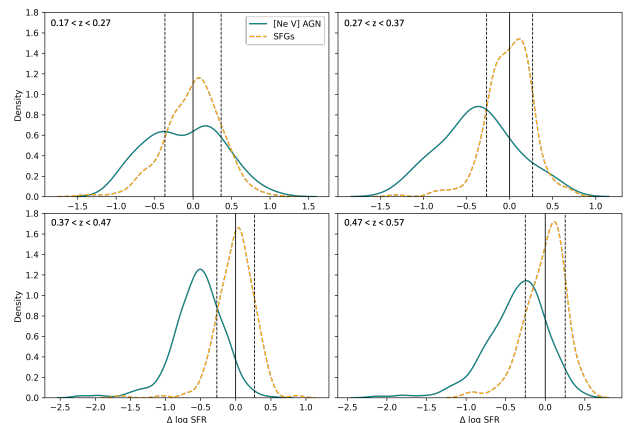


Figure 5. Redshift dependent plots showing the deviation from the MS. The MS as well as the $[\text{Ne v}]$ AGN are plotted in ranges of 0.1 in redshift, from 0.17 to 0.57. The deviation from the main sequence is clear in all plots, with the caveat of the small $[\text{Ne v}]$ sample size in the first. This demonstrates that there is no clear redshift dependence.

mass of the central SMBH (Ferrarese 2002; Bandara et al. 2009), strong $[\text{Ne v}]$ would preferentially occur in the higher mass galaxies. Unfortunately, this introduces a dichotomy between the masses of the SFGs and the $[\text{Ne v}]$ AGN. This implies that it is statistically impossible to differentiate between the deviation from the main sequence being applicable to high mass galaxies or to AGN specifically.

The lack of overlap in mass means that we can only investigate the deviation from the main sequence at fixed mass for one range, between $\log M_* = 10$ -10.5 for both our $[\text{Ne v}]$ AGN, and the full AGN sample. Performing a partial correlation test on this full AGN sub-sample, we find that there is a very low correlation between the SFR and the mass of the galaxy ($r = 0.02$), while there is

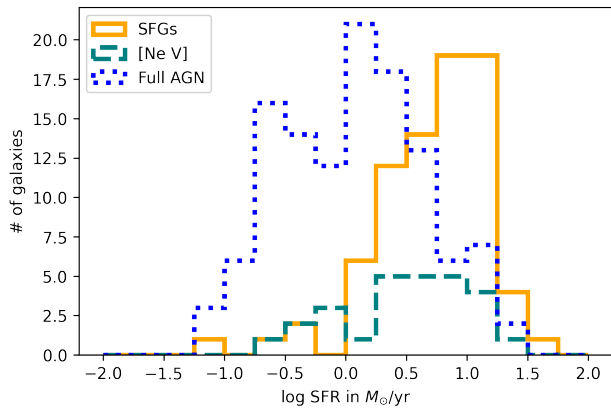


Figure 6. This plot shows the distribution of the SFRs for the SFGs, the [Ne v] AGN, and the full AGN sample within the restricted mass range of $\log M_* = 10\text{-}10.5$ (see Section 2 for sample descriptions). This shows once again that the AGN tend towards having lower SFRs compared to the SFGs, even within a fixed mass range.

a high correlation between the SFR and the galaxy type ($r = 0.36$). We also plot the distributions of the SFRs in Figure 6, which clearly shows the full AGN sample falling below the SFGs, as well as the [Ne v] AGN to a smaller extent.

3.4. Comparison With Previous Main Sequences

In addition to the standard MS plotting the SFR against the galaxy mass, we also investigate the sSFR MS and compare our distribution to previously determined main sequence regression lines. In Figure 7, we compare relationships found in Speagle et al. (2014) and Shimizu et al. (2015) to our SFGs and [Ne v] AGN data. These relationships have been calculated to specifically fit SFGs, without the influence of AGN.

The Speagle et al. (2014) relationship was obtained by combining a large number of MS fits found in the literature at a range of redshifts. The resulting relationship is thus time-dependent and is defined as:

$$\log \text{SFR}(M_*, t) = (0.96 - 0.045t) \log M_* - (7.41 - 0.27t) \quad (5)$$

where $\text{SFR}(M_*, t)$ is the star formation rate as a function of M_* , the mass of the galaxy in units of solar masses (M_\odot), and the time t , which corresponds to the age of the universe in Gyr. For our analysis, we further convert the time dependence in Equation 5 to a redshift one using the following equation:

$$t(z) = \frac{2}{3H_0\Omega_0^{1/2}(1+z)^{3/2}} \quad (6)$$

where t is again the age of the universe in Gyr, z is the redshift, $H_0 = 70.0 \text{ km s}^{-1} \text{ Mpc}^{-1}$, and $\Omega_0 = 0.721$ as

previously stated. The slope and intercept of the main sequence both go down as t increases or as z decreases. This is the case as the SFR is higher in younger galaxies. In Figure 7, we plot the relationship at a redshift of $z = 0.25$ which is close to the average redshift of our samples.

The Shimizu et al. (2015) relationship is, however, only dependent on galaxy mass as they used exclusively local ($z \leq 0.05$) galaxies. It is calculated as the best-fit line to *Herschel* Reference Survey and *Herschel* Stripe 82 survey data:

$$\log \text{SFR}(M_*) = 1.01 * \log M_* - 9.87 \quad (7)$$

where the variables are the same as in Equation 5. As implicitly shown in this equation, the slope of the sSFR MS relationship from the Shimizu et al. (2015) paper will be flat. It is clear by looking at Figure 7 that a flat relationship does not fit with our data. This is perhaps due to the inclusion of lower mass galaxies in the *Herschel* sample and possible biases in the BAT sample being hard X-ray selected.

However, as seen in Figure 7, our specific star formation main sequence plot trends are in overall agreement with the redshift-dependent relationship of Speagle et al. (2014), having a similar downward trending slope⁵. We can also see that there is a noticeable decrease in the sSFR with increasing mass in the [Ne v] sample. This trend is not as pronounced in the SFG sample, which suggests that the trend is affected by the presence of the AGN.

Our analysis is complementary to BAT sample analysis by Shimizu et al. (2015), as we both use a specific criterion to unambiguously target AGN. Our results regarding the AGN deviation from the main sequence support the ones found by Shimizu et al. (2015) despite the lack of overlap between our galaxies and the BAT sample, with the BAT AGN having a maximum redshift of $z = 0.05$. Being able to use the optical [Ne v] line as opposed to X-ray-selected AGN makes the result more accessible since it increases the possibility of detecting fainter objects.

4. DISCUSSION

In the previous section, we found that a significant percentage of the [Ne v] AGN fall below the star-forming main sequence, indicating a decrease in SFR at higher masses. This deviation from the main sequence has been used as an indicator of feedback in AGN, with the AGN causing the suppression of star formation via

⁵ The Speagle slope fits more closely with our MS when including a similar mass range as in their paper and removing outliers.

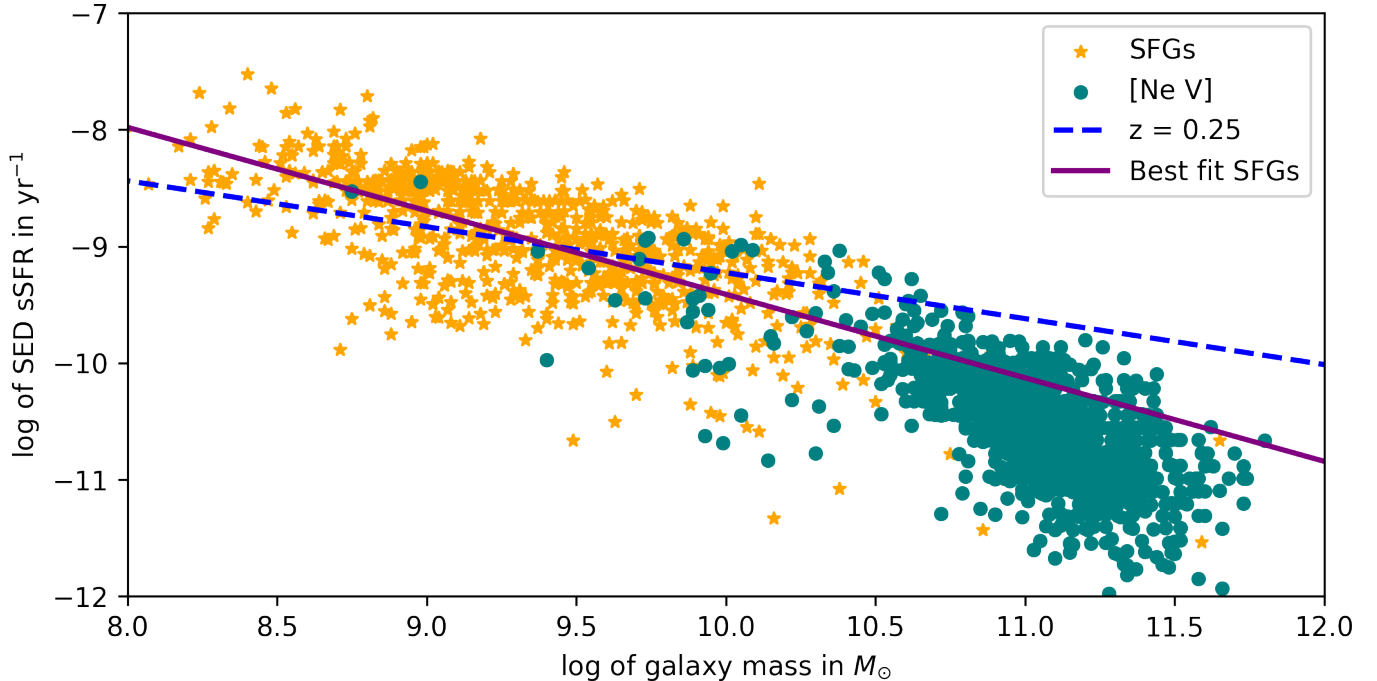


Figure 7. Comparing our sSFR MS (purple, solid) for our SFGs and [Ne v] AGN, with the relationship found in Speagle et al. (2014) for $z = 0.25$ (blue, dashed). We find that our SFG data fits well with the Speagle et al. (2014) relationships, which span a similar range in redshift as our SFGs. However, the [Ne v] AGN have a much steeper slope than the Speagle et al. (2014) lines, indicating once again a deviation from the MS.

various processes. In this section, we further investigate this possibility by looking at the bolometric luminosity of our [Ne v] AGN.

We calculated the bolometric luminosity (L_{bol}) for the galaxies in the [Ne v] sample using both the [O III] and the [Ne v] luminosities ($L_{[OIII]}$ and $L_{[NeV]}$). We used the [O III] bolometric correction for reddening corrected fluxes from Lamastra et al. (2009), which corresponds to multiplying $L_{[OIII]}$ by a factor of 454. Although different factors are suggested depending on the $L_{[OIII]}$ range, we decided to apply a single correction factor instead of differentiating between the AGN above and below the $\log L_{[OIII]} = 42$ threshold, as doing so created an artificial gap in the resulting plot. Additionally, 87% of the sample lies above the $\log L_{[OIII]} = 42$ limit.

We also used the relationship from Satyapal et al. (2007):

$$\log L_{bol} = 0.94 * \log L_{[NeV]_{IR}} + 6.32 \quad (8)$$

where L_{bol} is the bolometric luminosity, and $L_{[NeV]_{IR}}$ is the luminosity of the IR [Ne v] $14.32 \mu\text{m}$ line. We used a [Ne v] $14.32 \mu\text{m}$ /[Ne v] 3426 \AA ratio of 1.60 to calculate the bolometric luminosity using the optical [Ne v] line instead. The ratio was obtained using the Cloudy photoionization modeling code (v. 17.0, Ferland et al. 2017). The parameters used are the same as those outlined in Feuillet et al. (2024). However, we use a $\log U = -1.1$

to -1.3 and $\log n_H = 3 \text{ cm}^{-3}$ and averaging the results. We used a higher ionization parameter than in the previous models as we set out to optimize the parameters for [Ne v] emission (Ferguson et al. 1997). The two L_{bol} values follow a similar trend with an offset of about half an order of magnitude and have a general overlap.

Looking at the resulting plot containing both the [O III] and [Ne v] based bolometric luminosities, we see that neither appears to increase monotonically in any significant way (see Figure 8). Such an increase would have been expected as the mass of the galaxy is proportional to the mass of the central SMBH (Ferrarese 2002; Bandara et al. 2009). A higher mass SMBH would also be related to an increase in the amount of radiation for a given accretion rate, and thus increase the L_{bol} of the AGN. This result leaves us with two options. The first assumes that [O III] is a good measure of bolometric luminosity, which would indicate that the decrease in sSFR does not have anything to do with the strength of the AGN, as we would have otherwise expected L_{bol} to increase with the mass of the galaxy.

The second option would be that [O III] is not a good measure of bolometric luminosity. One possibility is that it could be due to over-ionization (Baldwin 1977). As [O III] is a measure of the ionizing radiation if over-ionized the resulting gas would be transparent and would not be able to re-radiate the entirety of the ioniz-

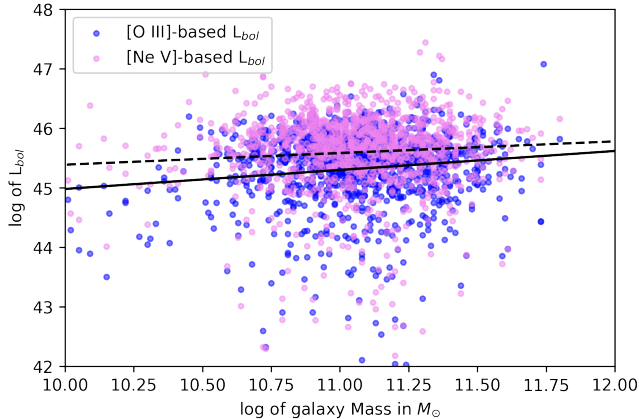


Figure 8. Bolometric luminosities for the [Ne v] sample obtained using two methods reliant on [O III] and [Ne v] respectively. The [O III]-based bolometric luminosity is calculated using the 454 factor from [Lamastra et al. \(2009\)](#). The [Ne v] bolometric luminosity uses both the relationship between L_{bol} and the luminosity of the IR [Ne v] 14.32 μm line from [Satyapal et al. \(2007\)](#), as well as a conversion factor between the IR and optical [Ne v] lines extracted from the previously used NLR Cloudy models. The solid and dashed black lines represent the line of best fit of the [Ne v]- and [O III]-based bolometric luminosities respectively.

ing radiation. It would theoretically be possible for the [Ne v] to also be over-ionized, but is unlikely given its high ionization potential. Therefore, the lack of divergence between the [O III] and [Ne v] determined bolometric luminosities suggests that over-ionization is not the most likely explanation.

The other reason would be a lack of gas in the galaxy. For example, the galaxy could have gone through a blowout stage, during which AGN feedback, or some other mechanism (e.g. [Heckman & Best 2014](#)), ejects gas from the host galaxy. Assuming that a majority of the AGN in our sample are past this blowout stage, this would explain both the decrease in sSFR and "specific bolometric luminosity". Indeed, there would not be enough gas to continue forming stars nor would there be as much left to ionize into [O III]. In agreement with other papers, our results do not suggest current AGN activity being responsible for the decrease in the SFR, but rather residual or reactivated AGN activity after the feedback has already ceased ([Peng et al. 2010](#); [Mulcahey et al. 2022](#); [Harrison et al. 2023](#)). The fact that we can see the deviation from the main sequence for the BAT, [Ne v], and OHNO AGN, spanning redshifts up to 1.06 indicates that the blowout phase must have occurred before then.

Another indication of this explanation arose when we looked at the SFR distributions for our samples and

compared them to those of [Shimizu et al. \(2015\)](#) in Figure 4. They each represent a different redshift span, with the BAT sample being local ($z \leq 0.05$), our SFGs and [Ne v] AGN ranging between $0.168 \leq z \leq 0.568$, and the OHNO AGN having redshifts from 0.568 to 1.07. The local MS showed that the SFR for the SFGs range between ≈ -1.5 to $0.5 \log \text{SFR}$, while the BAT AGN span from ≈ -1 to 1.5 . Our SFGs have an SFR range that is overall 1 dex higher than the local galaxies. This can be explained by the fact that the galaxies in our sample live closer to the peak in SFR, which occurred between $2 < z < 3$, with a sharp decline of about 1 dex from $z = 1$ and $z = 0$ ([Hopkins & Beacom 2006](#)).

However, the BAT AGN, our [Ne v]-selected AGN, and the OHNO AGN all appear to have almost identical ranges of SFR, despite representing different redshift ranges. The process responsible for the reactivation of the AGN would be also fueling the star formation within the galaxy, keeping the SFR constant over the range in redshift.

5. CONCLUSION

By applying several criteria to the full galaxy sample, we separated it into a SFG and a [Ne v] AGN sample in order to investigate their differences in behavior along the galaxy main sequence.

1. We calculated the specific SFR using three different methods: SED fitting provided by the Portsmouth group, [O II]-based sSFR using the relationship in [Kewley et al. \(2004\)](#), and $\text{H}\alpha$ -based from [Kennicutt \(1998\)](#). While all three methods gave consistent results for the SFG sample, the emission-line methods overestimated the SFRs of the AGN sample compared to the SED fitting values. Despite the limitations of both methods, we opted to use SED fitting values for both samples.
2. We plotted the MS for our SFG and [Ne v] AGN samples, and found that there is a deviation when it comes to the AGN. While only 15% of the SFGs fall below the MS, 49% of the [Ne v] AGN sample lies under, which indicates a reduction in SFR in almost half of the galaxies. This result is in agreement with that of [Shimizu et al. \(2015\)](#), which used the BAT AGN sample.
4. We also plotted the specific SFR MS and compared our data to previously determined MS relationships. Our data agrees well with the work of [Speagle et al. \(2014\)](#). We found a rapid decrease in sSFR in the AGN that is not as pronounced in SFGs, again suggesting a decrease in SFR with increasing mass in AGN.

5. We looked at the bolometric luminosity of our [Ne v] AGN sample using two different methods and found that the bolometric luminosity does not have a mass dependence. One possible explanation is that the deviation is due to a reduction in the SF in the AGN as a result of past activity. However, we cannot reach a definite conclusion with this data set.

This work has made use of SDSS DR12 data. Funding for the Sloan Digital Sky Survey IV has been provided by the Alfred P. Sloan Foundation, the U.S. Department of Energy Office of Science, and the Participating Institutions. SDSS-IV acknowledges support and resources from the Center for High Performance Computing at the University of Utah. The SDSS website is www.sdss4.org. The authors would like to thank the Portsmouth Group for making their data tables available online. The data can be found at https://www.sdss4.org/dr12/spectro/galaxy_portsmouth/.

REFERENCES

- Abel, N. P., & Satyapal, S. 2008, *ApJ*, 678, 686, doi: [10.1086/529013](https://doi.org/10.1086/529013)
- Alam, S., Albareti, F. D., Allende Prieto, C., et al. 2015, *ApJS*, 219, 12, doi: [10.1088/0067-0049/219/1/12](https://doi.org/10.1088/0067-0049/219/1/12)
- Baldwin, J. A. 1977, *ApJ*, 214, 679, doi: [10.1086/155294](https://doi.org/10.1086/155294)
- Baldwin, J. A., Phillips, M. M., & Terlevich, R. 1981, *PASP*, 93, 5, doi: [10.1086/130766](https://doi.org/10.1086/130766)
- Bandara, K., Crampton, D., & Simard, L. 2009, *ApJ*, 704, 1135, doi: [10.1088/0004-637X/704/2/1135](https://doi.org/10.1088/0004-637X/704/2/1135)
- Cao, C., Xia, X. Y., Wu, H., et al. 2008, *MNRAS*, 390, 336, doi: [10.1111/j.1365-2966.2008.13747.x](https://doi.org/10.1111/j.1365-2966.2008.13747.x)
- Cardelli, J. A., Clayton, G. C., & Mathis, J. S. 1989, *ApJ*, 345, 245, doi: [10.1086/167900](https://doi.org/10.1086/167900)
- Cid Fernandes, R., Stasińska, G., Mateus, A., & Vale Asari, N. 2011, *MNRAS*, 413, 1687, doi: [10.1111/j.1365-2966.2011.18244.x](https://doi.org/10.1111/j.1365-2966.2011.18244.x)
- Ciesla, L., Charmandaris, V., Georgakakis, A., et al. 2015, *A&A*, 576, A10, doi: [10.1051/0004-6361/201425252](https://doi.org/10.1051/0004-6361/201425252)
- Collins, N. R., Kraemer, S. B., Crenshaw, D. M., Bruhweiler, F. C., & Meléndez, M. 2009, *ApJ*, 694, 765, doi: [10.1088/0004-637X/694/2/765](https://doi.org/10.1088/0004-637X/694/2/765)
- Davies, R. L., Kewley, L. J., Ho, I. T., & Dopita, M. A. 2014, *MNRAS*, 444, 3961, doi: [10.1093/mnras/stu1740](https://doi.org/10.1093/mnras/stu1740)
- Di Matteo, T., Springel, V., & Hernquist, L. 2005, *Nature*, 433, 604, doi: [10.1038/nature03335](https://doi.org/10.1038/nature03335)
- Ferguson, J. W., Korista, K. T., Baldwin, J. A., & Ferland, G. J. 1997, *ApJ*, 487, 122, doi: [10.1086/304611](https://doi.org/10.1086/304611)
- Ferland, G. J., Chatzikos, M., Guzmán, F., et al. 2017, *RMxAA*, 53, 385. <https://arxiv.org/abs/1705.10877>
- Ferrarese, L. 2002, *ApJ*, 578, 90, doi: [10.1086/342308](https://doi.org/10.1086/342308)
- Feillet, L. M., Meléndez, M., Kraemer, S., et al. 2024, *The Astrophysical Journal*, 962, 104, doi: [10.3847/1538-4357/ad1a09](https://doi.org/10.3847/1538-4357/ad1a09)
- Gilli, R., Vignali, C., Mignoli, M., et al. 2010, *A&A*, 519, A92, doi: [10.1051/0004-6361/201014039](https://doi.org/10.1051/0004-6361/201014039)
- Goulding, A. D., & Alexander, D. M. 2009, *MNRAS*, 398, 1165, doi: <https://doi.org/10.1111/j.1365-2966.2009.15194.x>
- Harrison, C. M., Girdhar, A., & Ward, S. R. 2023, arXiv e-prints, arXiv:2307.03770, doi: [10.48550/arXiv.2307.03770](https://doi.org/10.48550/arXiv.2307.03770)
- Heckman, T. M., & Best, P. N. 2014, *ARA&A*, 52, 589, doi: [10.1146/annurev-astro-081913-035722](https://doi.org/10.1146/annurev-astro-081913-035722)
- Hopkins, A. M., & Beacom, J. F. 2006, *ApJ*, 651, 142, doi: [10.1086/506610](https://doi.org/10.1086/506610)
- Kennicutt, R. C. 1998, *Annual Review of Astronomy and Astrophysics*, 36, 189, doi: [10.1146/annurev.astro.36.1.189](https://doi.org/10.1146/annurev.astro.36.1.189)
- Kennicutt, R. C., & Evans, N. J. 2012, *Annual Review of Astronomy and Astrophysics*, 50, 531, doi: [10.1146/annurev-astro-081811-125610](https://doi.org/10.1146/annurev-astro-081811-125610)
- Kewley, L. J., Geller, M. J., & Jansen, R. A. 2004, *AJ*, 127, 2002, doi: [10.1086/382723](https://doi.org/10.1086/382723)
- King, A. 2003, *ApJL*, 596, L27, doi: [10.1086/379143](https://doi.org/10.1086/379143)

- Lamastra, A., Bianchi, S., Matt, G., et al. 2009, *A&A*, 504, 73, doi: [10.1051/0004-6361/200912023](https://doi.org/10.1051/0004-6361/200912023)
- Leslie, S. K., Kewley, L. J., Sanders, D. B., & Lee, N. 2016, *MNRAS*, 455, L82, doi: [10.1093/mnras/slv135](https://doi.org/10.1093/mnras/slv135)
- Madau, P., & Dickinson, M. 2014, *Annual Review of Astronomy and Astrophysics*, 52, 415, doi: [10.1146/annurev-astro-081811-125615](https://doi.org/10.1146/annurev-astro-081811-125615)
- Maraston, C., Daddi, E., Renzini, A., et al. 2006, *ApJ*, 652, 85, doi: [10.1086/508143](https://doi.org/10.1086/508143)
- Maraston, C., Pforr, J., Henriques, B. M., et al. 2013, *MNRAS*, 435, 2764, doi: [10.1093/mnras/stt1424](https://doi.org/10.1093/mnras/stt1424)
- McPartland, C., Sanders, D. B., Kewley, L. J., & Leslie, S. K. 2019, *MNRAS*, 482, L129, doi: [10.1093/mnras/sly202](https://doi.org/10.1093/mnras/sly202)
- Meléndez, M., Heckman, T. M., Martínez-Paredes, M., Kraemer, S. B., & Mendoza, C. 2014, *MNRAS*, 443, 1358, doi: [10.1093/mnras/stu1242](https://doi.org/10.1093/mnras/stu1242)
- Meléndez, M., Kraemer, S. B., Schmitt, H. R., et al. 2008, *ApJ*, 689, 95, doi: [10.1086/592724](https://doi.org/10.1086/592724)
- Mignoli, M., Vignali, C., Gilli, R., et al. 2013, *A&A*, 556, A29, doi: [10.1051/0004-6361/201220846](https://doi.org/10.1051/0004-6361/201220846)
- Mulcahey, C. R., Leslie, S. K., Jackson, T. M., et al. 2022, *A&A*, 665, A144, doi: [10.1051/0004-6361/202142215](https://doi.org/10.1051/0004-6361/202142215)
- Mullaney, J. R., Alexander, D. M., Aird, J., et al. 2015, *MNRAS*, 453, L83, doi: [10.1093/mnras/slv110](https://doi.org/10.1093/mnras/slv110)
- Noeske, K. G., Weiner, B. J., Faber, S. M., et al. 2007, *ApJL*, 660, L43, doi: [10.1086/517926](https://doi.org/10.1086/517926)
- Pacifici, C., Iyer, K. G., Mobasher, B., et al. 2023, *The Astrophysical Journal*, 944, 141, doi: [10.3847/1538-4357/acacff](https://doi.org/10.3847/1538-4357/acacff)
- Peng, Y.-j., Lilly, S. J., Kovač, K., et al. 2010, *ApJ*, 721, 193, doi: [10.1088/0004-637X/721/1/193](https://doi.org/10.1088/0004-637X/721/1/193)
- Salim, S., Rich, R. M., Charlot, S., et al. 2007, *ApJS*, 173, 267, doi: [10.1086/519218](https://doi.org/10.1086/519218)
- Salpeter, E. E. 1955, *ApJ*, 121, 161, doi: [10.1086/145971](https://doi.org/10.1086/145971)
- Sarzi, M., Falcón-Barroso, J., Davies, R. L., et al. 2006, *MNRAS*, 366, 1151, doi: [10.1111/j.1365-2966.2005.09839.x](https://doi.org/10.1111/j.1365-2966.2005.09839.x)
- Satyapal, S., Vega, D., Dudik, R. P., Abel, N. P., & Heckman, T. 2008, *ApJ*, 677, 926, doi: [10.1086/529014](https://doi.org/10.1086/529014)
- Satyapal, S., Vega, D., Heckman, T., O'Halloran, B., & Dudik, R. 2007, *ApJ*, 663, L9, doi: [10.1086/519995](https://doi.org/10.1086/519995)
- Schmidt, M., Hasinger, G., Gunn, J., et al. 1998, *A&A*, 329, 495. <https://arxiv.org/abs/astro-ph/9709144>
- Shimizu, T. T., Mushotzky, R. F., Melendez, M., Koss, M., & Rosario, D. 2015, *MNRAS*, 452, 1841, doi: [10.1093/mnras/stv1407](https://doi.org/10.1093/mnras/stv1407)
- Silk, J., & Rees, M. J. 1998, *A&A*, 331, L1, doi: [10.48550/arXiv.astro-ph/9801013](https://doi.org/10.48550/arXiv.astro-ph/9801013)
- Speagle, J. S., Steinhardt, C. L., Capak, P. L., & Silverman, J. D. 2014, *ApJS*, 214, 15, doi: [10.1088/0067-0049/214/2/15](https://doi.org/10.1088/0067-0049/214/2/15)
- Stemo, A., Comerford, J. M., Barrows, R. S., et al. 2020, *The Astrophysical Journal*, 888, 78, doi: [10.3847/1538-4357/ab5f66](https://doi.org/10.3847/1538-4357/ab5f66)
- Thomas, A. D., Kewley, L. J., Dopita, M. A., et al. 2018, *ApJL*, 861, L2, doi: [10.3847/2041-8213/aacce7](https://doi.org/10.3847/2041-8213/aacce7)
- Thomas, D., Steele, O., Maraston, C., et al. 2013, *Monthly Notices of the Royal Astronomical Society*, 431, 1383, doi: [10.1093/mnras/stt261](https://doi.org/10.1093/mnras/stt261)
- Torbaniuk, O., Paolillo, M., Carrera, F., et al. 2021, *MNRAS*, 506, 2619, doi: [10.1093/mnras/stab1794](https://doi.org/10.1093/mnras/stab1794)
- Zhuang, M.-Y., & Ho, L. C. 2019, *ApJ*, 882, 89, doi: [10.3847/1538-4357/ab340d](https://doi.org/10.3847/1538-4357/ab340d)